THREE-GOLD CLUSTER AS PROTON ACCEPTOR IN NONCONVENTIONAL HYDROGEN BONDS O-H...Au AND N-H...Au

2 AUTHORS:

Eugene S Kryachko
University of Liège
139 PUBLICATIONS **2,031** CITATIONS

SEE PROFILE

F. Remacle
University of Liège
185 PUBLICATIONS **3,530** CITATIONS

SEE PROFILE

Three-gold clusters form nonconventional hydrogen bonds O–H···Au and N–H···Au with formamide and formic acid

E.S. Kryachko [a,b,*], F. Remacle [a,*,1]

[a] *Department of Chemistry, Bat. B6c, University of Liège, Sart-Tilman, B-4000 Liège, Belgium*
[b] *Bogoliubov Institute for Theoretical Physics, Kiev 03143, Ukraine*

Abstract

The complexes between triangle three-gold cluster and formamide and formic acid are studied within high-level density functional and MP2 approaches. The most stable ones are planar and cyclic, and formed via the Au–O anchor and N–H···Au or O–H···Au bonds for formamide and formic acid, respectively. These N–H···Au and O–H···Au bonds satisfy all the conditions required to identify conventional hydrogen bonds and can thus be treated as new, nonconventional H-bonds. Their formation is based on the cooperativity of the involved molecular interactions where the Au–O anchor bond plays a leading role. The corresponding H-bonds with Ag_3 are found to be weaker.
© 2005 Elsevier B.V. All rights reserved.

1. Introduction

The concept of hydrogen bonds A–H···B as the bond formed between a proton donor group A–H and a proton acceptor B containing lone-pair electrons is well accepted and widely used in many areas of physics, chemistry, and biology (see [1–11] and references therein). The definition of conventional hydrogen or H-bonds states that a hydrogen bond A–H···B, geometrically characterized by the bond lengths $R(A–H)$ and $r(H···B)$ and the bond angle $\angle AHB$, is formed iff the following conditions are satisfied [1–11]:

(i) there exists a clear evidence of the bond formation – this might be, e.g., the appearance of the H-bond stretching mode $v_\sigma(A···B)$;

(ii) there exists a clear evidence that this bond specifically involves a hydrogen atom which is bonded to B predominantly along the bond direction A–H (see particularly [10,11]);

(iii) the A–H bond elongates relative to that in the monomer;

(iv) the hydrogen bond separation $r(H···B)$ defined as the distance between the bridging proton and the proton acceptor B is shorter than the sum of van der Waals radii of H and B, that is, the so called van der Waals cutoff (see particularly [5,6,8] and note [21] in Ref. [10]); $r(H···B) < w_H + w_B$, where w_X is the van der Waals radius of X. The distance $r(A···B)$ between the proton donor, A, and the proton acceptor, B, is often referred to as the H-bond length. The necessary but insufficient condition imposed on $r(A···B)$ indicating that the H-bond is formed is that $r(A···B) < w_A + w_B$;

(v) the stretching vibrational mode $v(A–H)$ undergoes a red shift with respect to that in the isolated A–H group and its IR intensity significantly increases;

* Corresponding authors. Fax: +32 4 366 3413.
  E-mail addresses: eugene.kryachko@ulg.ac.be (E.S. Kryachko), fremacle@ulg.ac.be (F. Remacle).
  [1] Maître de Recherche, FNRS, Belgium.

(vi) proton nuclear magnetic resonance (^{1}H NMR) chemical shifts in the A–H···B hydrogen bond are shifted downfield compared to the monomer.

Note that the conditions **(iii)**–**(vi)** can also be treated as an indirect justification of validity of **(ii)**.

Within the hydrogen bonding theory [1–11], the atoms F, N, O, C, P, S, Cl, Se, Br, and I have lone-pair electrons. They play the role of typical conventional proton acceptors which participate in the formation of conventional hydrogen bonds.

It has been recently reported that the family of proton acceptors can be extended to some transition metals which are capable of forming nonconventional hydrogen bonds [12–15]. The aim of the present work is to show that gold can also play the role of a proton acceptor and form nonconventional hydrogen bonds with conventional proton donors, such as the O–H and N–H groups. In particular, our high level ab initio computations demonstrate that the most stable, planar, cyclic complexes between a three-gold cluster and formamide and formic acid are formed via two different kinds of bonds: one of the gold atoms is anchored to the carbonyl oxygen and another one either to the amino group of formamide or to the hydroxyl group of formic acid via the bonds N–H···Au and O–H···Au, respectively. We argue that these H-bonds share all the common features **(i)**–**(vi)** of conventional hydrogen bonds and can hence be considered as nonconventional H-bonds.

2. Computational methodology

All computations of the complexes formamide–Au_3 and formic acid–Au_3 were conducted using the GAUSSIAN03 package of quantum chemical programs [16]. The Kohn–Sham self-consistent field formalism was used together with the hybrid density functional B3LYP potential and relativistic effective core potential (RECP) for the gold atoms. The basis set is defined as 6-31++G(d,p) for the formamide and formic acid and by the RECP for gold. Three different energy-consistent 19-$5s^2 5p^6 5d^{10} 6s^1$ valence-electron RECPs for gold were chosen: the RECP of Ermler, Christiansen and co-workers (EC) [17], of the Stuttgart group (S) [18], and of Hay

and Wadt (Los Alamos, or shortly HW-LA) [19] (for recent applications to gold clusters see [20,21] and references therein). All geometrical optimizations were carried out with the keywords 'tight' and 'Int = UltraFine'. The harmonic vibrational frequencies, zero-point vibrational energies (ZPVE), and enthalpies were also calculated. The reported binding energies include the ZPVE correction. The B3LYP/6-31++G(d,p) computational approach provides an accurate description of the properties of formamide (FO) [22,23] and formic acid (FA) [24,25]. Their properties relevant to the present study are given in Table 1. One of the studied complexes, formic acid–Au_3, was also investigated at second-order Møller–Plesset perturbation level MP2/HW-LA (gold) ∪6-31++G(d,p).

3. Existence of N–H···Au and O–H···Au hydrogen bonds: A computational proof

The most stable planar complexes between a three-gold cluster and either formamide or formic acid are reported in Fig. 1. This Figure shows that Au_3 forms with FO an anchor Au–O bond that is shorter (by about 0.03 Å for all used RECPs) and hence stronger than the one formed with FA. This is one of the reasons why FO–Au_3 is energetically more stable, by ca. 3 kcal mol^{-1}, than FA–Au_3 (see Table 2 for a list of the key features of both complexes; note that the binding energy of the complex FA–Au_3 amounts to 17.5 kcal mol^{-1} at the MP2/HW-LA (gold) ∪6-31++G(d,p) (formic acid) level). The anchoring of the Au_3 cluster to the carbonyl oxygen of formamide or formic acid goes together with the formation of N–H···Au and O–H···Au bonds. Our purpose is to show that these intramolecular bonds share the features typical of the conventional hydrogen bond [1–11]. In order to do so, we systematically review below the necessary and sufficient conditions **(i)**–**(vi)** for the FO–Au_3 and FA–Au_3 complexes.

Condition **(i)**: the existence of the N_2–H_2···Au_5 and O_2–H_2···Au_5 bonds in FO–Au_3 and FA–Au_3, respectively, is confirmed by the appearance of the stretching modes $v_\sigma(N_2 \cdots Au_5)$ in FO–Au_3 and $v_\sigma(O_2 \cdots Au_5)$ in FA–Au_3, whose frequencies fall within the range of 133–142 cm^{-1} depending on the RECP. These modes

Table 1
Some key features of monomers, formamide (FO) and formic acid (FA), computed at the B3LYP/6-31++G(d,p) level

FO	FA
$r(C_1–N_2) = 1.361$, $r(C_1{=}O_3) = 1.219$, $r(N_2–H_2') = 1.008$,	$r(C_1–O_2) = 1.347$, $r(C_1{=}O_3) = 1.207$, $r(O_2–H_2) = 0.974$,
$r(N_2–H_2) = 1.011$, $r(C_1–H_1) = 1.106$, $\angle C_1 N_2 H_2 = 119.3°$	$r(C_1–H_1) = 1.098$, $\angle C_1 N_2 H_2 = 107.9°$
$v(N_2–H_2, H_2') = 3587$ ($A_{IR} = 36$) and 3732 ($A_{IR} = 45$)	$v(O_2–H_2) = 3732$ ($A_{IR} = 60$)
$v(N_2–D_2, H_2') = 2662$ ($A_{IR} = 35$) and 3679($A_{IR} = 45$)	$v(O_2–D_2) = 2714$ ($A_{IR} = 40$)
$\sigma_{iso}(N_2) = 163.2$, $\sigma_{iso}(H_2) = 26.9$, $\sigma_{an}(N_2) = 123.1$, $\sigma_{an}(H_2) = 9.8$	$\sigma_{iso}(O_2) = 134.8$, $\sigma_{iso}(H_2) = 25.4$, $\sigma_{an}(O_2) = 190.2$, $\sigma_{an}(H_2) = 9.5$

Bond lengths are given in Å, vibrational frequencies in cm^{-1}, IR activities, A_{IR}, in km mol^{-1}, and $\delta\sigma_{iso}$ and $\delta\sigma_{an}$ in ppm.
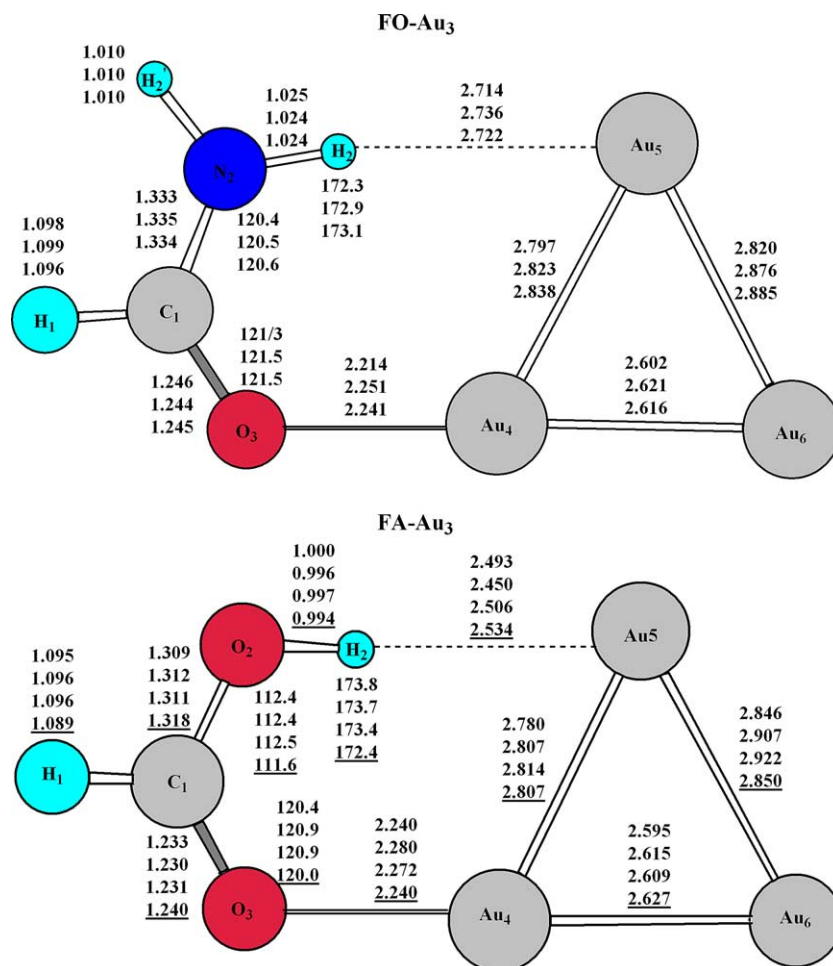
Fig. 1. The most stable FO–Au$_3$ and FA–Au$_3$ complexes computed at the B3LYP/RECP (gold) ∪6-31++G(d,p) (formamide and formic acid) level. The bond lengths are given in Å and bond angles in deg (reading from top to bottom: RECP = EC, S, HW-LA). The bottom line of data (underlined) for the complex FA–Au$_3$ corresponds to the MP2/HW-LA (gold) ∪6-31++G(d,p) (formic acid) computational level.

Table 2
Some key features of the most stable complexes FO–Au$_3$ and FA–Au$_3$ which exhibit nonconventional H-bonds N–H···Au and O–H···Au, respectively

	FO–AU$_3$			FA–Au$_3$		
	EC	S	HW-LA	EC	S	HW-LA
E_b	17.2	16.1	14.9	14.4	13.2	12.0
$-\Delta H_f$	17.2	16.1	15.0	14.3	13.0	11.8
v(X–H)	3366 (363)	3387 (323)	3388 (327)	3212 (879)	3279 (830)	3263 (849)
$-\Delta v$(X–H)	221	200	199	520	453	463
v(X–D)	2476 (222)	2492 (202)	2493 (204)	2340 (544)	2389 (483)	2377 (497)
$-\Delta v$(X–D)	186	170	169	374	325	337

The binding energy E_b (including zero-point vibrational energy, in kcal mol^{-1}) and the enthalpy, $-\Delta H_f$ (kcal mol^{-1}), of formation are defined with respect to the infinitely separated monomers (FO or FA and Au$_3$ cluster).
Δv(X–H) in cm^{-1}, X = N (FO–Au$_3$) and O (FA–Au$_3$).
The stretching frequencies are supplied with their IR activities A_{IR} (in km mol^{-1}, in parentheses).
The three columns for each complex correspond to the values obtained with the three RECPs: EC, S, and HW-LA.

are coupled to the stretching mode of Au$_4$–O$_3$ anchor bond.

Regarding the conditions (iii)–(vi), it is seen from Table 2 and Table 3 that they are satisfied for the N$_2$–H$_2$···Au$_5$ and O$_2$–H$_2$···Au$_5$ bonds in the complexes FO–Au$_3$ and FA–Au$_3$, respectively. In addition, since their bond angles are close to π ($\angle$N$_2$H$_2$Au$_5$ = 172.3–173.1° and $\angle$O$_2$H$_2$Au$_5$ = 173.4–173.8°, at the MP2/HW-LA(gold) ∪6-31++G(d,p) (formic acid) level, the H-bond angle $\angle$O$_2$H$_2$Au$_5$ = 172.4°; see Fig. 1), these

Table 3
Parameters relevant to conditions (iii)–(vi) for the FO–Au$_3$ and FA–Au$_3$ complexes computed at B3LYP/RECP (gold) $\cup$6-31++G(d,p) (FO and FA) level

Condition	FO–Au$_3$	FA–Au$_3$
(iii)	$\Delta R(N_2–H_2) = 0.013–0.014$ Å	$\Delta R(O_2–H_2) = 0.023–0.026$ Å
(iv)	$r(H_2\cdots Au_5) = 2.714–2.736$ Å	$r(H_2\cdots Au_5) = 2.450–2.506$ Å
(v)	$-\Delta v(N_2–H_2) = 199–221$ cm^{-1}	$-\Delta v(O_2–H_2) = 453–520$ cm^{-1}
	$A_{IR}(N_2–H_2\cdots Au_5)/A_{IR}(N_2–H_2) = 9–10$	$A_{IR}(O_2–H_2\cdots Au_5)/A_{IR}(O_2–H_2) = 14–15$
	$-\Delta v(N_2–D_2) = 169–186$ cm^{-1}	$-\Delta v(O_2–D_2) = 325–374$ cm^{-1}
	$A_{IR}(N_2–D_2\cdots Au_5)/A_{IR}(N_2–D_2) = 5–6$	$A_{IR}(O_2–D_2\cdots Au_5)/A_{IR}(O_2–D_2) = 12–14$
(vi)	$\delta\sigma_{iso}(H_2) = -3.0$ to -3.4 ppm	$\delta\sigma_{iso}(H_2) = -3.5$ to -4.1 ppm
	$\delta\sigma_{iso}(N_2) = -22.7$ to -24.3 ppm	$\delta\sigma_{iso}(O_2) = -35.6$ to -41.3 ppm
	$\delta\sigma_{an}(H_2) = 9.2–9.7$ ppm	$\delta\sigma_{an}(H_2) = 13.3–14.4$ ppm
	$\delta\sigma_{an}(N_2) = -18.6$ to -20.0 ppm	$\delta\sigma_{an}(O_2) = -75.0$ to -82.2 ppm

ΔR(A–H) is the elongation of the A–H bond with respect to the corresponding monomer.
Δv(A–H) is the shift of the stretching mode v(A–H) taken with respect to the corresponding monomer and A_{IR} stands for the IR activity.
$\delta\sigma_{iso}$ and $\delta\sigma_{an}$ (both in ppm) are taken with respect to the corresponding monomers, see Table 1.

two bonds are almost linear. Inspecting Tables 2 and 3, we find that:

Condition (iii): The bond O$_2$–H$_2$ in FA–Au$_3$ is more elongated (almost by factor of two) than the N$_2$–H$_2$ in FO–Au$_3$. The MP2/HW-LA (gold) $\cup$6-31++G(d,p) (formic acid) predicts the elongation of the O$_2$–H$_2$ bond of FA–Au$_3$ as equal to $\Delta R(O_2–H_2) = 0.021$ Å;

Condition (iv): For the two complexes, the bond length $r(H\ldots Au) < w_H + w_{Au} = 2.86$ Å (at the MP2/HW-LA (gold) $\cup$6-31++G(d,p) (formic acid), $r(H_2\cdots Au_5) = 2.534$ Å). Note also the hydrogen bond in FA–Au$_3$ is shorter and thus stronger than in FO–Au$_3$, which implies that the bridging proton is better shared in the latter complex, even though the former is more stable;

Condition (v): The red shifts undergone by the stretching modes when the hydrogen bonds are formed mirror the trend in the strength of H-bond already mentioned in (iii) and (iv). It is worth mentioning that the MP2/HW-LA (gold) $\cup$6-31++G(d,p) (formic acid) level predicts $\Delta v(O_2–H_2) = -422$ cm^{-1} and $A_{IR}(O_2–H_2\cdots Au_5)/A_{IR}(O_2–H_2) = 12$. Table 3 also includes the data on red shifts and IR activity for the isotopomers FO and FA with H$_2$ being replaced by D$_2$;

Condition (vi): The changes in the NMR chemical shift of the bridging proton resulting from the formation of the hydrogen bonding-type interaction are a well-known key indicator of the hydrogen bond formation (vi) (see also [26–28]). For the studied complexes, $\delta\sigma_{iso}(H_2)$ is negative, as it should be if a hydrogen bond is formed because its formation in the FO–Au$_3$ and FA–Au$_3$ induces a deshielding of the bridging proton. The $\delta\sigma_{iso}(H_2)$ is more negative, by ~-0.5 to -0.7 ppm, for FA–Au$_3$. This reflects again the stronger character of its H-bond. Moreover, the reported shifts $\delta\sigma_{iso}(H_2)$ are below the $\delta\sigma_{iso}(H) = -2.8$ ppm of the bridging proton in water dimer [28]. The range of the anisotropic shifts $\delta\sigma_{an}(H_2)$ is much wider that for the isotropic ones. For FA–Au$_3$, it is larger than

that of water dimer (=11.2 ppm) but equal to those of water chains (H$_2$O)$_{4-5}$ [28].

The features reported in Table 3 show that the bonds N$_2$–H$_2$$\cdots$Au$_5$ and O$_2$–H$_2$$\cdots$Au$_5$, formed in the complexes FO–Au$_3$ and FA–Au$_3$, respectively, are nonconventional H-bonds. We suggest that these nonconventional H-bonds belong to the class of so called 'anchor-assisted' hydrogen bonds since the complexes are unstable unless the anchoring bond is formed. For example, the complex FO–Au$_3$ where the gold cluster is attached to H$_2'$ (see Fig. 1) by H-bonding only is unstable. There is a substantial charge redistribution that is induced by the formation of the Au–O anchor bond. For example, the Mulliken atomic charges of FA–Au$_3$, computed at the B3LYP/HW-LA (gold) $\cup$6-31++G(d,p) (FA) level, undergo the following changes relative to those in the monomers: $\Delta q(C_1) = 0.092$, $\Delta q(O_2) = 0.029$, $\Delta q(H_2) = 0.235$, $\Delta q(O_3) = 0.041$, $\Delta q(Au_4) = 0.047$, $\Delta q(Au_5) = -0.297$, and $\Delta q(Au_6) = -0.195$. The charge redistribution strengthens the proton acceptor ability of the gold atom, Au$_5$, that is provided by its lone-pair-like 5d orbital. Actually, there exists a back 'donation' from these nonconventional H-bonds to the corresponding anchor ones via either the FO or the FA backbone, respectively, that illustrates the cooperativity of the involved molecular interactions. This back 'donation' mechanism leads to a shortening of the carbonyl bond and to a lengthening of the C–N bond in FO or of the C–O bond in FA. To summarize, a cooperative 'feedback mechanism' drives the electron density flow and thus governs the formation of both bonds. However, being stronger and partially covalent, the anchor bond plays a dominant role. As a result of its formation, additional negative charge accumulates on the nonconventional H-bond acceptor, the gold atom Au$_5$, that causes a partial lengthening (and thus weakening) of the two Au–Au bonds between Au$_5$ and the atoms Au$_4$ (by 0.13–0.17 Å) and Au$_6$ (by 0.19–0.28 Å). However, while the complex FO–Au$_3$ is stronger than FA–Au$_3$, its nonconventional hydrogen bond is

weaker. This is due to the fact that the deprotonation enthalpy of the conventional donor group N_2–H_2 of formamide, equal to 359.8 ± 2.1 kcal mol^{-1} [29], is larger than that (345.3 ± 2.2 kcal mol^{-1} [30]) of the donor group O_2–H_2 of formic acid. Therefore, the former is less perturbed by the gold cluster compared to the latter.

In general, the data collected in (iii)–(iv) can be used to estimate the strength of the hydrogen bond which is usually expressed in terms of the H-bond formation energy E_{HB}. This is obviously not possible here because of the presence of the anchor bond. Nevertheless, the strength of the H-bonds in FO–Au_3 and FA–Au_3 can be estimated because formamide and formic acid can form other, less stable complexes with Au_3 where there is no H-bond. These are the complexes where Au_3 anchors the same oxygen atom as in those of Fig. 1, but is structurally placed on the C_1–H_1 side, so that the formation of a H-bond with the N_2–H_2 of formamide or with the O_2–H_2 of formic acid is prevented. The geometries of these less stable complexes, FO–Au_3^{trans} and FA–Au_3^{trans}, are shown in Fig. 2. The difference in energy between FO–Au_3 and FO–Au_3^{trans} amounts to 3.3–3.6 kcal mol^{-1}. This represents about 21% of the total binding energy of FO–Au_3 and hence corroborates the

above assumption on the leading role of the anchor bonding in the cooperative feedback mechanism governing the stabilization of this complex. The difference in energy between FA–Au_3 and FA–Au_3^{trans} is larger and varies within 4.4–5.1 kcal mol^{-1}, that is about 35% of the total binding energy of FA–Au_3. Provided that other structural differences between FO–Au_3 and FO–Au_3^{trans}, and between FA–Au_3 and FA–Au_3^{trans} are neglected (The most noteworthy structural differences are predicted for the anchor bonds: in FO–Au_3 and FA–Au_3, they are shorter by 0.03 and 0.05 Å, respectively, compared to FO–Au_3^{trans} and FA–Au_3^{trans}), these energies provide reasonable upper-bound estimates of the strengths of the hydrogen bonds N–H$\cdots$Au in FO–Au_3 and O–H$\cdots$Au in FA–Au_3: $-E_{HB}(N_2$–$H_2\cdots Au_5) \leqslant 3.3$ to 3.6 kcal mol^{-1} and $-E_{HB}(O_2$–$H_2\cdots Au_5) \leqslant 4.4$ to 5.1 kcal mol^{-1}. A comparison of the Mulliken charges of the atoms O_2 and H_2 in the complexes FA–Au_3 and FA–Au_3^{trans} demonstrates a trend that is typical of conventional H-bonding interaction (see, in particular, [13]). The unconventional H-bond O_2–$H_2\cdots Au_5$ is formed upon the transition from FA–Au_3^{trans} to FA–Au_3. In the FA–Au_3 conformation, the bridging proton looses electron density and hence becomes more
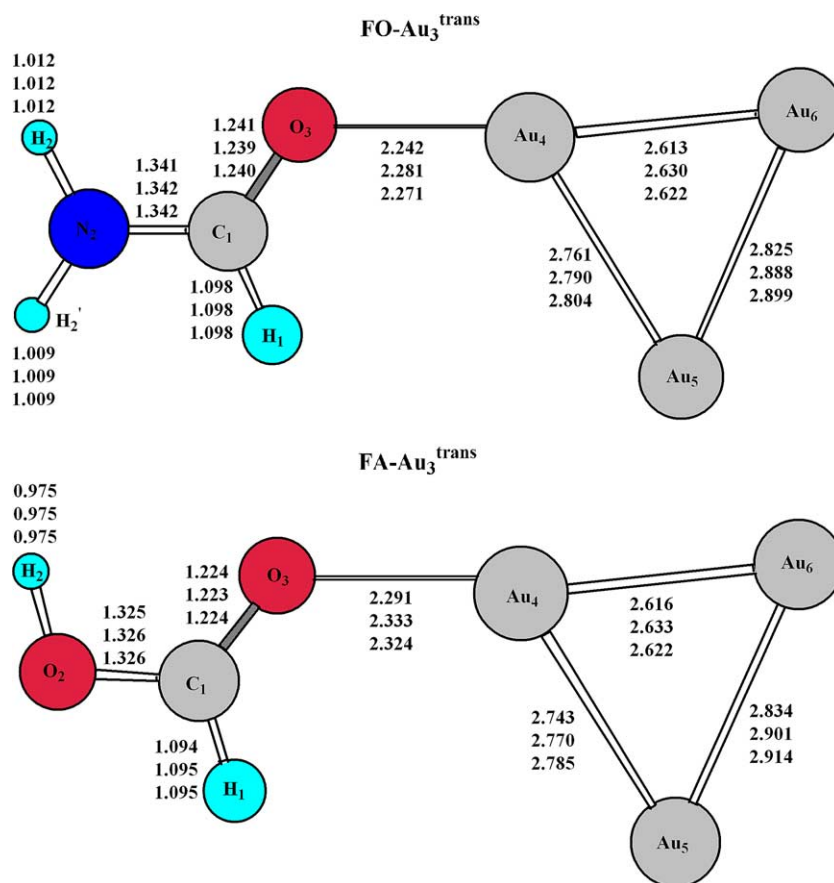

Fig. 2. The complexes FO–Au_3^{trans} and FA–Au_3^{trans} (same computational levels as in Fig. 1). The bond lengths are given in Å and bond angles in degrees (reading from top to bottom: RECP = EC, S, HW-LA).
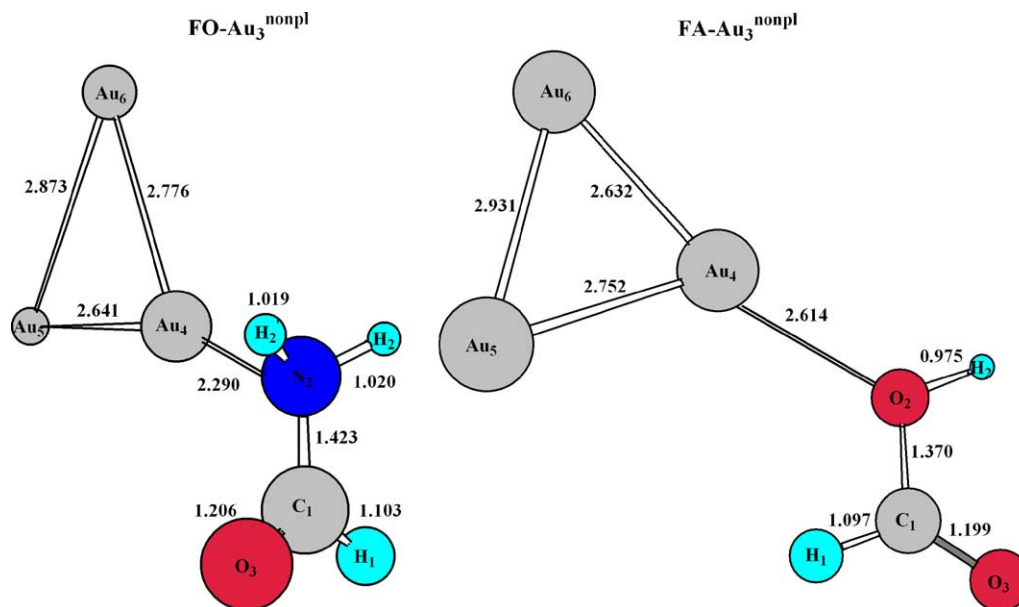
Fig. 3. The complexes FO–Au$_3^{nonpl}$ and FA–Au$_3^{nonpl}$ (B3LYP/HW-LA (gold) $\cup$6-31++G(d,p) (formamide and formic acid)). The bond lengths are given in Å and bond angles in degrees.

positively charged by 0.221. This occurs simultaneously with a charge transfer between the conventional proton donor O_2 and the unconventional proton acceptor Au_5 that causes a larger negative charge (by -0.015) on O_2. By analogy with [13], the negative Mulliken charge of Au_5 also increases by -0.095, mostly by draining the electron density from the $C_1=O_2$–Au_4 bond.

Three more points are worth discussing before closing this Section. First: The anchoring of a three-gold cluster to the N_2 atom in FO–Au$_3$ and to O_2 atom of FA–Au$_3$ results in the nonplanar complexes, FO–Au$_3^{nonpl}$ and FA–Au$_3^{nonpl}$, drawn in Fig. 3. Their anchor bonds are longer than those in FX–Au$_3$ and FX–Au$_3^{trans}$ (X = O, A) and therefore, these nonplanar complexes are weaker: FO–Au$_3^{nonpl}$ is weaker by 7.2 kcal mol^{-1} than FO–Au$_3$ and FA–Au$_3^{nonpl}$ by 9.1 kcal mol^{-1} than FA–Au$_3$ (RECP = HW-LA). Second: So far, we have suggested a cooperative feedback mechanism that drives the electron charge flow and governs the formation of the Au–O anchor bonds in the planar complexes FO–Au$_3$ and FA–Au$_3$. Within the three-gold cluster, this strengthens the proton acceptor ability of one of its unanchored gold atom. The lone-pair-like 5d orbital of this gold atom allows an electron density to flow to the conventional proton donor and the bridging proton. Another example that supports this mechanism and particularly emphasizes the cooperativity of involved molecular interactions is shown in Fig. 4 where the complex FA–Au$_3^{trans} - w$, obtained at the B3LYP/HW-LA (gold) $\cup$6-31++G(d,p) (formic acid and water) computational level is plotted. In this complex, the water molecule accepts one H-bond C_1–$H_1 \cdots$ O_7 from formic acid and donates another, C_1–

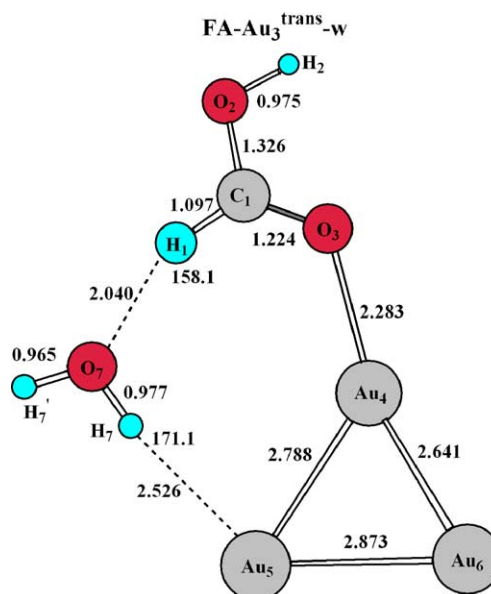Fig. 4. The complex FA–Au$_3^{trans} - w$ obtained at the B3LYP/HW-LA (gold) $\cup$6-31++G(d,p) (formic acid, water) computational level. The bond lengths are given in Å and bond angles in degrees.

$H_1 \cdots Au_5$, to the gold cluster. The former is known to be very weak (see, e.g., [8]) and this is indicated by a small lengthening of the C_1–H_1 bond by 0.002 Å and a small red-shift of the C_1–H_1 stretch equal to 30 cm^{-1}. The other H-bond is a weak nonconventional hydrogen bond since, its O_7–H_7 bond elongates by 0.012 Å; the $v(O_7$–$H_7)$ downshifts by 208 cm^{-1}; and its IR activity increases by a factor of almost 11. The binding energy of FA–Au$_3^{trans} - w$, taken with respect to the infinitely separated FA–Au$_3^{trans}$ and water molecule, amounts to
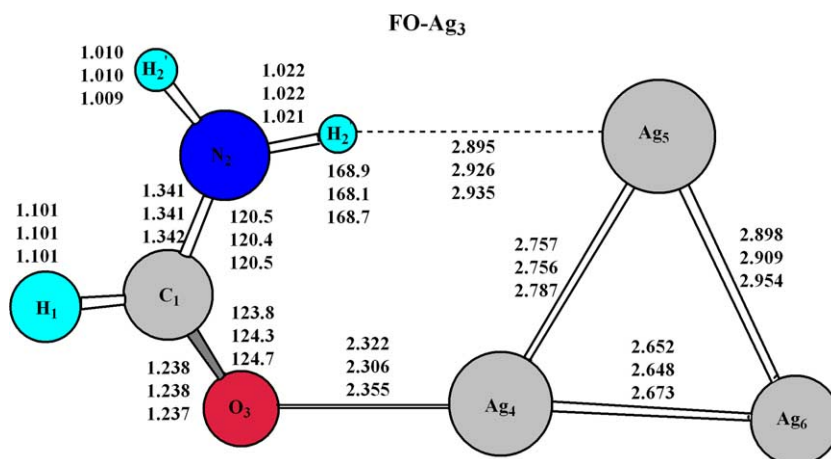
Fig. 5. The most stable FO–Ag$_3$ complex (B3LYP/HW-LA (Ag) ∪6-31++G(d,p)). The bond lengths are given in Å and bond angles in degrees (reading from top to bottom: RECP = EC, S, HW-LA).

7.0 kcal mol^{-1}. This value also gives a reasonable estimate of the strength of the nonconventional hydrogen bond O–H⋯Au that is formed in the complex with FA–Au$_3^{trans}$ − w, even though some corrections due to the geometrical relaxation of the monomer FA–Au$_3^{trans}$, mainly occurring in the vicinity of the anchor bond Au–O (which itself is contracted by 0.041 Å) should be taken into account. The third point is whether a silver cluster Ag$_3$ behaves similarly to Au$_3$. Fig. 5 and Table 4 provide answers to this question. The bond N–H⋯Ag in FO–Ag$_3$ is weaker than the N–H⋯Au that is found in FO–Au$_3$. Strictly speaking, the condition (iv) is only weakly satisfied. However, according to [5,6,8,10] (see particularly [21] in [10]), the van der Waals cutoff is a too strong criterion. It should be extended to 3.0 Å, or even to 3.2 Å. Provided this extension, the N–H⋯Ag bond can be treated as a nonconventional hydrogen bond. We suggest that two factors are mainly responsible for its weakness: first, the lower polarizability of Ag$_3$ compared to that of Au$_3$ and second, the 4d orbitals of

Ag are spatially less extended than the gold 5d ones and hence, they are less involved in the electron density flow that accompanies the formation of the H-bond and determines its strength.

To conclude, this work presents computational evidence of the ability of a triangle three-gold cluster to behave as a nonconventional proton acceptor and to form nonconventional H-bonds with conventional proton donors. This is illustrated by the hydrogen bonds N–H⋯Au and O–H⋯Au, that are, respectively, formed between Au$_3$ and formamide and formic acid. The mechanism behind their formation depends on the formation of the dominating Au–O anchor bond that causes substantial charge redistributions within the FO–Au$_3$ and FA–Au$_3$ complexes. In turn, this electron flow strengthens the proton acceptor ability of the gold atom Au$_5$.

Table 4
Conditions (iii)–(vi) for the FO–Ag$_3$ complex within the B3LYP/RECP (silver) ∪6-31++G(d,p) (formamide) approaches

Condition	FO–Ag$_3$
(iii)	ΔR(N$_2$–H$_2$) = 0.010–0.011 Å
(iv)	r(H$_2$⋯Ag$_5$) = 2.895–2.935 Å (w_H + w_{Ag} = 2.92 Å)
(v)	$-\Delta v$(N$_2$–H$_2$) = 162–178 cm^{-1}
	A_{IR}(N$_2$–H$_2$⋯Ag$_5$)/A_{IR}(N$_2$–H$_2$) = 9–10
	$-\Delta v$(N$_2$–D$_2$) = 142–154 cm^{-1}
	A_{IR}(N$_2$–D$_2$⋯Ag$_5$)/A_{IR}(N$_2$–D$_2$) = 6–7
(vi)	$\delta\sigma_{iso}$(H$_2$) = −2.2 to −2.4 ppm
	$\delta\sigma_{iso}$(O$_2$) = −19.4 to −20.3 ppm
	$\delta\sigma_{an}$(H$_2$) = 5.6–5.9 ppm
	$\delta\sigma_{an}$(O$_2$) = −15.1 to −16.5 ppm

ΔR(N$_2$–H$_2$) is the elongation of the N$_2$–H$_2$ bond in FO–Ag$_3$ with respect to that in formamide.
Δv(N$_2$–H$_2$) is the shift of the stretching mode v(N$_2$–H$_2$) taken with respect to formamide and A_{IR} stands for the IR activity.

References

[1] D. Haždi, H.W. Thompson (Eds.), Hydrogen Bonding, Pergamon Press, London, 1959.

[2] C.G. Pimentel, A.L. McClellan, The Hydrogen Bond, Freeman, San Francisco, 1960.

[3] W.C. Hamilton, J.A. Ibers, Hydrogen Bonding in Solids, Benjamin, New York, 1968.

[4] P. Schuster, G. Zundel, C. Sandorfy (Eds.), The Hydrogen Bond, Recent Developments in Theory and Experiments, North-Holland, Amsterdam, 1976.

[5] G.A. Jeffrey, W. Saenger, Hydrogen Bonding in Biological Structures, Springer, Berlin, 1991.

[6] G.A. Jeffrey, An Introduction to Hydrogen Bonding, Oxford University Press, Oxford, 1997.

[7] S. Scheiner, Hydrogen Bonding, A Theoretical Perspective, Oxford University Press, Oxford, 1997.

[8] G.R. Desiraju, T. Steiner, The Weak Hydrogen Bond in Structural Chemistry and Biology, Oxford University Press, Oxford, 1999.

[9] P. Schuster, in: B. Pullman (Ed.), Intermolecular Interactions: from Diatomics to Biopolymers, Wiley, Chichester, 1978, p. 363.

[10] T. Steiner, Angew. Chem. Int. Ed. 41 (2002) 48.

[11] T. Steiner, G.R. Desiraju, Chem. Commun. 891 (1998).

[12] E.S. Shubina, N.V. Belkova, L.M. Epstein, J. Organomet. Chem. 17 (1997) 536.

[13] G. Orlova, S. Scheiner, Organometallics 17 (1998) 4362.

[14] L.M. Epstein, E.S. Shubina, Coord. Chem. Rev. 231 (2002) 165, and references therein.

[15] L. Brammer, Dalton Trans. (2003) 3145, and references therein.

[16] M.J. Frisch et al., GAUSSIAN03, Revision A.1, Gaussian Inc., Pittsburgh, PA, 2003.

[17] R.B. Ross, J.M. Powers, T. Atashroo, W.C. Ermler, L.A. LaJohn, P.A. Christiansen, J. Chem. Phys. 93 (1990) 6654.

[18] D. Andrae, U. Haeussermann, M. Dolg, H. Stoll, H. Preuss, Theor. Chim. Acta 77 (1990) 123.

[19] P.J. Hay, W.R. Wadt, J. Chem. Phys. 82 (1985) 270, 299.

[20] F. Remacle, E.S. Kryachko, Adv. Quantum Chem. 47 (2004) 423.

[21] F. Remacle, E.S. Kryachko, J. Chem. Phys. 122 (2005) 044304.

[22] D.P. Chong, P. Aplincourt, C. Bureau, J. Phys. Chem. A 106 (2002) 356, and references therein.

[23] G.V. Papamokos, I.N. Demetropoulos, J. Phys. Chem. A 108 (2004) 7291, and references therein.

[24] J.H. Lim, E.K. Lee, Y. Kim, J. Phys. Chem. 101 (1997) 2233, and references therein.

[25] D. Wei, J.-F. Truchon, S. Sirois, D. Salahub, J. Chem. Phys. 116 (2002) 6028, and references therein.

[26] J.F. Hinton, K. Wolinski, in: D. Haždi (Ed.), Theoretical Treatments of Hydrogen Bonding, Wiley, Chichester, 1997, p. 75.

[27] E.D. Becker, in: D.M. Grant, R.K. Harris (Eds.), Encyclopedia of Nuclear Magnetic Resonance, Wiley, New York, 1996, p. 2409.

[28] T. Kar, S. Scheiner, J. Phys. Chem. A 108 (2004) 9161, and references therein.

[29] R.W. Taft, Prog. Phys. Org. Chem. 16 (1987) 1.

[30] G. Caldwell, R. Renneboog, P. Kebarle, Can. J. Chem. 67 (1989) 661.